ISOTROPICALLY-ETCHED MICROBALL BEARING SYSTEMS

B. Hanrahan[1,2], S. Misra[1], J. Feldman[1], C. M. Waits[2], and R. Ghodssi[1]
[1]MEMS Sensors and Actuators Laboratory (MSAL)
Department of Electrical and Computer Engineering, Institute for Systems Research, Department of Materials Science and Engineering University of Maryland, College Park, MD 20742, USA
[2]U.S. Army Research Laboratory, Adelphi, MD 20783, USA

Abstract: Deep-groove raceway geometries are used in macro-scale rolling bearings to accommodate combination thrust and high-speed-induced radial loads. An improved plasma-based microfabrication technique has been developed to obtain the first-ever deep-groove (circular cross-sectioned) microball bearing raceways. Deep-groove raceways have been employed in the fabrication and operation of ball-bearing supported microturbines. A multi-step inductively coupled plasma (ICP)-based method was created to obtain deep-groove geometry with less than 2% deviation amongst intended raceway depth, width, and curvature. Etching depth uniformity was measured to be 0.15% within the raceway of a single device. Additionally, the ball contact angle has been simulated for the designed geometry and confirmed experimentally. The deep-groove bearing geometry has been demonstrated within a microturbine to speeds in excess of 65 krpm, and the failure mode has been shown to correlate with simulations.

Keywords: DRIE, Isotropic etching, Microball bearings

INTRODUCTION

Rolling bearings are an essential component of modern machinery, providing low friction and wear contact between moving parts. Specialized bearings are employed depending on their specific application, based on load, speed, and geometric requirements. Rolling bearing technology has been extended to the realm of micro-electromechanical systems (MEMS) in the demonstration of high-performance linear and rotary micro-machines. Proof-of-concept micromotors [1], microturbines [2], micropumps [3], and microgenerators [4], supported on microball bearings have all relied non-ideal planar geometries for their bearing raceways. Ghodssi *et al.* recently showed that future microfabricated bearing systems will need to accommodate for actuation-induced axial loads as well as inertia-induced radial loads, and will therefore require circular cross sectioned bearing structures to handle the resultant load [5]. This paper describes the development of a 3D etching technique used to obtain uniform, circular cross-sectioned bearing raceways and their utilization in the next generation rotary microsystems, allowing for stable high-speed

Future microball bearing utilizing systems, such as a microgenerator, will require high speeds. The top-down fabrication style of MEMS dictates the actuation mechanism, be it electrostatic, electromagnetic, or pneumatic will impart an axial (through wafer) load on the bearings. The centripetal force acting on the rotating balls will impart radial load scaling with the square of velocity, therefore radial forces on the ball bearing will need to be accounted for in addition to the thrust load. To accomplish this, a circular raceway cross-section is created. A schematic of the rectangular and circular bearings can be seen in Fig. 1.

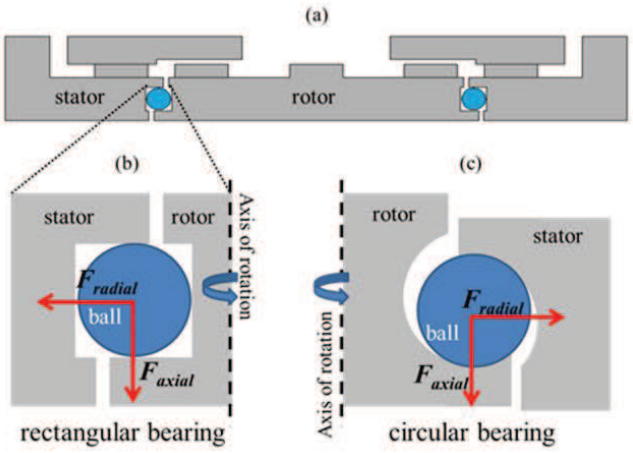

Fig. 1. Comparison of bearing geometries: (a) schematic of microturbine, (b) rectangular cross-section bearing defined by DRIE and used in previous microball bearing devices, (c) circular cross-sectioned bearing developed using custom isotropic etching techniques.

The bearing in Fig. 1a has been used in various microsystems and has shown consistent operation over 200 million revolutions at 10 krpm [5] and brief operation up to 87 krpm [3]. An ultimate limiting factor in the operation of a device with the rectangular geometry is the lack of ability to accommodate significant radial load. At low speeds the friction forces between the ball and raceway are capable of

restricting the ball radial motion. At high speeds, the centripetal forces overcome the friction forces and the ball begins make significant contact with the outer wall, ultimately resulting in a loss of rotor stability and failure. This concept is discussed theoretically in [5] and measured experimentally with on-chip accelerometers in [6].

DESIGN AND FABRICATION

The microturbine presented herein, as well as any number of rotary MEMS devices utilizing ball bearings in circular raceways can be fabricated using the scheme presented in Fig. 1. The microturbine is comprised of two wafers, bonded together encapsulating the ball bearings. The outer surfaces of the wafers contain the turbine structures patterned in a silicon dioxide hard mask for later use (Fig. 1a). The inner surfaces of the wafers contain the raceways defined in Fig. 2b and isotropically etched in Fig. 1c. The raceways also contain offset release structures that are defined by spray coat lithography and etched with DRIE to be accessed later (Fig. 1d). Bond alignment structures are also defined and etched during the spray-coat process on the inner surface of the two wafers. A shadow-masked evaporation of eutectic gold/tin is deposited on the inner surfaces of the wafers. Microball bearings are then placed in the etched raceways and the two wafers are bonded (Fig. 1e). Finally, the silicon dioxide hard mask patterned in Fig. 1a is utilized as a DRIE etch mask and the outer surfaces are etched make contact with the release etches, thereby releasing the rotor from the stator portions of the chip (Fig. 1f).

The most critical aspects of the fabrication are the geometry of the raceway and the location of the offset release etches. The etching techniques developed in this paper set forth the fabrication guidelines for obtaining circular raceways, proven with rotor diameters from 1mm to 10mm. The location of the offset release etch depends on the radius of the raceway, the geometry of the rotor, the expected centripetal load from the desired operating speeds, and the amount of thrust load tolerable. The resultant of the vector sum of radial and thrust loads gives the contact angle between the ball and raceway. The offset release etch trench on the thrust (non-turbine structured) side of the rotor is radially further from the axis of rotation than center of the raceway.

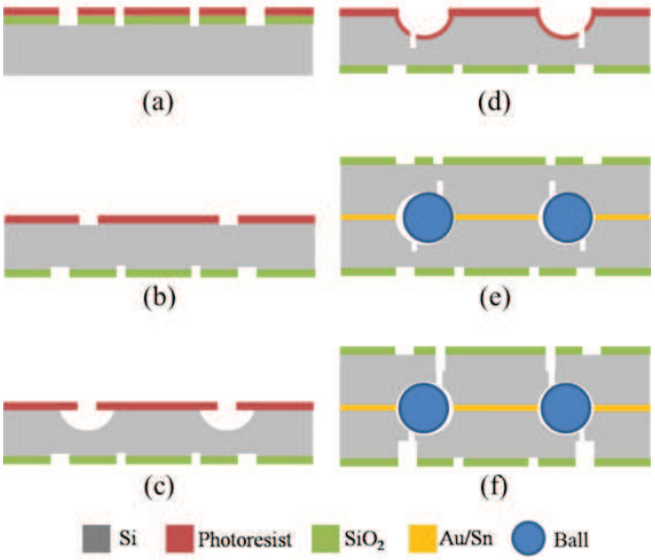

Fig. 2. Fabrication scheme for rotary MEMS with circular raceways.

At increasing speeds and centripetal load the balls will push out radially, towards the thrust side release etch structures. The release should therefore be offset as much as possible until the point where it is so far offset that the rotor is no longer held into position by the balls and could be completely removed from the stator. A minimum allowable contact angle of 37° was selected based upon the contact area of the ball and the desired operating parameters. This angle then determines the maximum operating speed for a given normal load. Fig. 3 shows a numerical simulation of the ball contact angle over a range of speeds and normal loads, used to design the raceway geometry.

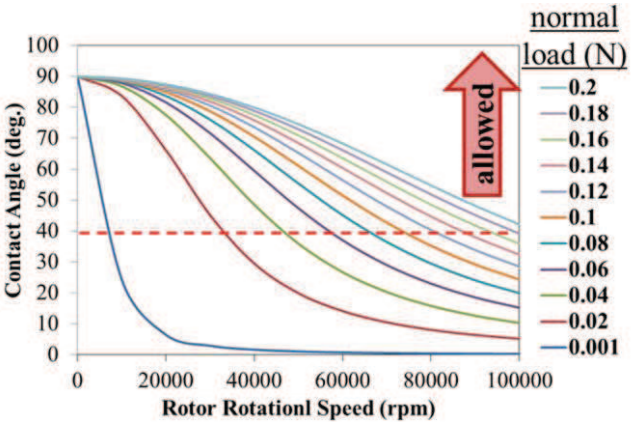

Fig. 3. Numerical simulation of contact angle for various loads and speeds.

RESULTS & DISCUSSION

Etch Experiments

A parametric study of the ICP etch was performed to obtain smooth raceways of the proper geometry. *Mask geometry, chamber pressure, plate power, and*

gas flow rates were optimized in a two-step etch process, inspired by the work reported by Larsen, *et al.* [7]. The first etch step defines the depth and a majority of the curvature. The second step is performed by selectively etching the reentrant profile formerly beneath the mask area after the etch mask is removed.

The selection of the correct masking geometry was the first challenge of the isotropic etching study. Through experiments of various mask opening geometries and knowledge of lateral and vertical etch rates, one obtains a mask opening of 230 µm needed for a ball with radius of 250 µm. Because the second step in the two-step process widens the raceway w/out etching vertically, the mask opening experiments were adjusted to be centered on a 200 µm opening.

Once the mask opening was determined, the bulk of the experiment was focused on the careful manipulation of the first plasma parameters in order to finely tune the raceway geometry. The plasma properties of interest were primarily the chamber pressure and RF plate power. Eight identical wafers were prepared with arrays of test raceways patterned with photolithography in 10 µm-thick AZ 9260 photoresist. Each wafer was etched for 65 min. to obtain near final dimensions. The parameters of interest were vertical and lateral etch rates, roughness, curvature, and photoresist selectivity.

Varying the RF plate power will change the strength of the magnetic field that directs the plasma ions to the surface of the substrate. In general, the ICP etching mechanism is a combination of chemical etching from the fluorination and subsequent volatilization of silicon, and physical etching from the sputtering of surface atoms by plasma ions. The range of plate powers tested (6-16 W) is not expected to produce ions with enough energy to overcome the 4.62 eV binding energy of silicon. This implies the etch process here is purely chemical and explains the consistent etch rates observed in the system, e.g., if higher plate powers increased the etch rate, then there would be some physical etching mechanism at play. The significant change in selectivity, however, shows that the masking material does undergo physical sputtering, and is therefore less effective at high plate powers. The reduction in curvature at higher powers can be explained by the enhanced density of ions delivered to the bottom of the trench versus the sidewalls by the increased directionality of the ion paths.

The physical implications of chamber pressure are complicated because of the competing effects of plasma density and a change in the mean-free-path (MFP) of the plasma molecule. Longer MFP ions travel further without a collision at lower pressures versus higher pressures, implying that the ions will have slightly more time to accelerate and will therefore hit the surface with a higher energy. Higher pressures may reduce the mean free path, but increase the plasma density and therefore the number of reactive species on the surface. The increased plasma density accelerates etching. The diameter of curvature obtained ranged from 422 – 532 µm as pressure was raised from 17 – 27 mTorr, which is expected based on the reduced directionality of ions in higher-pressure plasmas.

Fig. 4 shows the depth, width, and curvature evolutions of the tuned etch process.

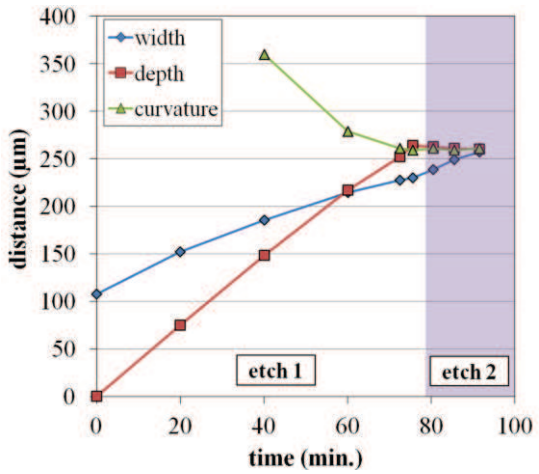

Fig. 4. Evolution of etch geometry through two-step ICP process. When width=depth=curvature, an ideal circular geometry has been obtained.

The bulk of the material is removed during the *etch 1* step and the curvature and depth nearly reach their final values. It is also interesting to note that there is some non-linearity in the lateral etch rate, with the etch slowing down towards the end of *etch 1*. This is a result of a minor starvation of reactants to the undercut sidewalls. Fig. 5 shows a completed raceway (half) and the theoretical placement of a ball.

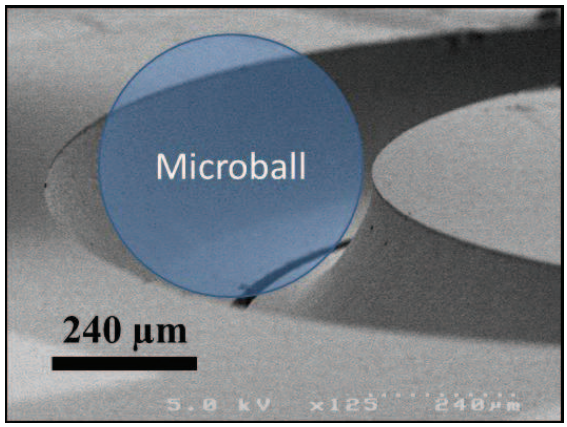

Fig. 5. SEM of completed raceway half with a microball schematically represented. Nested release etch is visible at the bottom of the raceway.

Microturbine Testing

Microturbine testing is performed by monitoring the turbine operating parameters: flow, pressure, and speed, through an acrylic package. A 5 mm rotor diameter, silicon carbide ball utilizing microturbine was tested (Fig. 6) as a first demonstration of this etch methodology. It was operated successfully above 65 krpm before catastrophic failure. The normal load on the rotor was 30 mN at 65 krpm, which resulted in a contact angle below 37°, allowing the ball to make contact with the offset release etch. It is assumed raceway facture was initiated at the sharp contact point where the offset etch meets the raceway. Once fracture was initiated on the raceway, the rotor became unstable and completely fractured the raceway over a time period of less than 10 seconds. Testing of this turbine was an experimental confirmation of the limits set forth from the numerical simulation. Actuation flow and thrust flow are controlled manually, therefore adjustments are made discretely and there is lag between adjustments and microturbine response. Future software control systems could integrate a contact angle calculator and adjust flows to maintain a desired contact angle for a given speed.

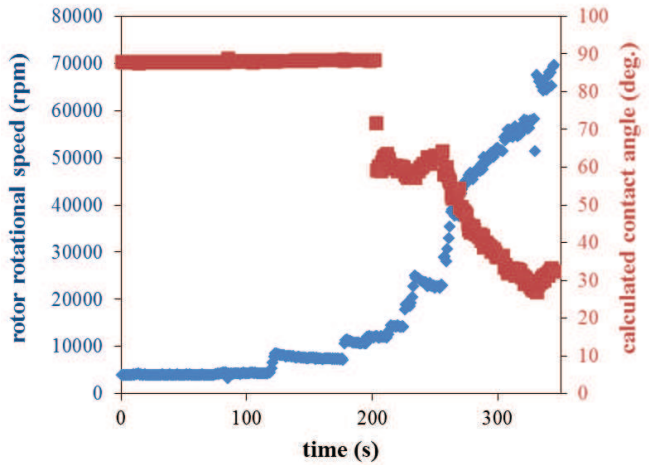

Fig. 6. Operation of the first isotropic bearing-containing microturbine. Showing measured rotor speed and calculated contact angle.

CONCLUSION

This paper presents the development of a 3D fabrication technique with the potential of significantly improving the performance of micro-scale rotary structures. The utilization of microball bearings for MEMS has shown great promise through an array of demonstrations, but there has always been a fundamental speed limit set by geometries limited by fabrication techniques. By developing a process to create uniform, smooth, curved surfaces, micro-scale ball bearings are enabled in regimes where load can be accommodated for both axially and radially. Deep-groove style ball bearings were selected to demonstrate the isotropic etch process within a functional device. Accordingly, a dynamic model of the bearing system was developed around a deep-groove style microfabricated geometry.

Macro-scale bearings universally utilize curved raceway surfaces to accommodate for combination thrust and radial loads. The curved surface allows for the area of contact to remain perpendicular to the ball axis of rotation through changing operating loads. This study presents the first demonstration of curved raceway surfaces within a micro-scale ball bearing system. Future high-performance microsystems utilizing ball bearings can use this technique to create stable, long-lived mechanical systems.

ACKNOWLEDGEMENTS

The authors would like to acknowledge the U.S. Army Cleanroom staff for their assistance with this work. This study was funded under National Science Foundation (NSF) award No. 0901411.

REFERENCES

[1] McCarthy M, Waits C M, Beyaz M I, Ghodssi R 2009 *J. of Micromechanics and Microengineering* **19** 094007.

[2] McCarthy M, Waits C M, Ghodssi R 2009 *J. of Microelectromechanical Systems* **18** 263-273.

[3] Waits C M, McCarthy M, Ghodssi R 2010 *J. of Microelectromechanical Systems* **19** 99-109.

[4] Beyaz M, Hanrahan B, Feldman J, Ghodssi R 2012 *Int. Conf. on MicroElectroMechanical Systems* 1209-1212.

[5] Ghodssi R, Hanrahan B, Beyaz M 2011 *16th Int. Conf. on Solid-State Sensors, Actuators, and Microsystems* 1789-1794.

[6] Hanrahan B, Feldman J, Misra S, Mitcheson P D, Waits C M, Ghodssi R 2012 *Int. Conf. on MicroElectroMechanical Systems* 579-582.

[7] Larsen K P, Ravnkilde J T, Hansen O 2005 *J. of Micromechanics and Microengineering,* **15** 873-882.